

# ChemComm

Chemical Communications

Accepted Manuscript

This article can be cited before page numbers have been issued, to do this please use: M. Upadhyay, R. Deka and D. Ray, *Chem. Commun.*, 2025, DOI: 10.1039/D5CC01970B.



This is an Accepted Manuscript, which has been through the Royal Society of Chemistry peer review process and has been accepted for publication.

Accepted Manuscripts are published online shortly after acceptance, before technical editing, formatting and proof reading. Using this free service, authors can make their results available to the community, in citable form, before we publish the edited article. We will replace this Accepted Manuscript with the edited and formatted Advance Article as soon as it is available.

You can find more information about Accepted Manuscripts in the [Information for Authors](#).

Please note that technical editing may introduce minor changes to the text and/or graphics, which may alter content. The journal's standard [Terms & Conditions](#) and the [Ethical guidelines](#) still apply. In no event shall the Royal Society of Chemistry be held responsible for any errors or omissions in this Accepted Manuscript or any consequences arising from the use of any information it contains.

## COMMUNICATION

## Charge Transfer Alteration and White Light Emission in Photochromic Triphenylamine-Norbornadiene-Triazine Switch

Manoj Upadhyay, Raktim Deka, and Debdas Ray\*

Received 00th January 20xx,  
Accepted 00th January 20xx

DOI: 10.1039/x0xx00000x

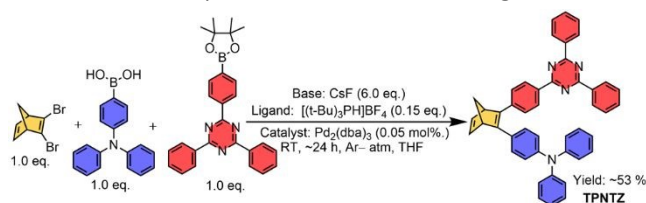
Herein, we present a photochromic compound that reversibly switches emission colour by adjusting its charge transfer pathway. Its reversible photoisomerization toggles charge transfer through bonds or space, controlling white light emission. Computational and photophysical studies highlight its promise for advanced optoelectronic applications.

Photochromic molecules change form in response to external stimuli and have been widely studied for use in data storage,<sup>1,2</sup> optical switching,<sup>3</sup> energy storage,<sup>4</sup> and light-controlled electronics.<sup>5</sup> Researchers have explored well-known photoswitchable molecules like hydrazones,<sup>6</sup> diarylethenes,<sup>7</sup> spiropyranes,<sup>8</sup> fulgides,<sup>9</sup> and azobenzenes,<sup>10</sup> for their reliable and reversible transformations. The norbornadiene-quadracycline (NBD-QC) couple stands out for solar energy storage,<sup>4</sup> molecular electronics,<sup>11</sup> and tunable photonics<sup>2,12</sup> due to its high-energy storage capacity, strong photostability, and rapid thermal reversibility. When NBD absorbs radiation, it undergoes an electrocyclic transformation to its metastable QC form, causing significant shifts in molecular geometry, conjugation, and electronic structure.<sup>4,13</sup> Over the past decade, researchers have developed donor-acceptor (D-A) systems for photovoltaics,<sup>14</sup> OLEDs,<sup>15</sup> bioimaging,<sup>16</sup> sensing, and nonlinear optics.<sup>17</sup> Controlling charge transfer (CT) in these systems is key to unlocking new applications.<sup>18</sup> Typically, in D-A systems, CT occurs via a through-bond charge transfer (TBCT) mechanism, where an extended  $\pi$ -system facilitates charge migration due to the delocalization of frontier molecular orbitals (FMO).<sup>19</sup> However, studies show that through-space charge transfer (TSCT) can also occur via non-covalent interactions,<sup>20</sup> especially in systems with steric hindrance, non-conjugated linkers, or molecular twisting.<sup>21</sup> The ability to switch between TBCT and TSCT in a single molecule holds promise for developing multifunctional optoelectronic materials. To this context, designing white light emitters remains challenging due to the

color balance.<sup>6,22</sup> Herein, we designed a donor-NBD-acceptor photochromic system that integrates a triphenylamine (TPA) donor and a triazine (TNZ) acceptor through a norbornadiene (NBD) bridge, forming **TPNTZ** (Fig. 1). The NBD/QC unit enables dynamic control of CT pathways under external light. In its initial NBD form, **TPNTZ** expected to exhibit more prominent TBCT due to partial conjugation between TPA and TNZ. Upon photoisomerization to the QC isomer (**TPQZ**), the molecular structure undergoes breaking of the conjugation, which leads to significant geometric distortion and increases the donor-acceptor separation. As a result, TBCT weakens while TSCT strengthens, leading to a shift in CT dynamics. UV-vis absorption analysis confirmed a reversible transformation between **TPNTZ** and **TPQZ** with excellent fatigue resistance. Emission studies showed **TPQZ** emits blue light, while **TPNTZ** emits orange in methylcyclohexane (MCH) solution, revealing distinct CT characteristics. By adjusting **TPNTZ** and **TPQZ** ratios by 365 nm light, we achieved white light emission. Quantum studies further validated the different extents of CT in **TPNTZ** and **TPQZ**. This work provides fundamental insights into the tunable CT properties of donor-NBD/QC-acceptor systems modulated by photo-switching of NBD/QC couple.

We synthesized **TPNTZ** using a one-step Suzuki coupling reaction,<sup>23</sup> where 2,3-dibromonorbornadiene was treated with (4-(diphenylamino)phenyl)boronic acid and 2,4-diphenyl-6-(4-(4,4,5,5-tetramethyl-1,3,2-dioxaborolan-2-yl)phenyl)-1,3,5-triazine simultaneously under inert atmosphere (Scheme 1). After purification by column chromatography, the yellow solid formed with a 53% yield. NMR spectroscopy, mass spectrometry, and X-ray crystallography confirmed its structure (ESI†).

X-ray analysis showed that triphenylamine donor and triphenyl-1,3,5-triazine acceptor attached to the NBD segment were

Scheme 1. Synthesis scheme of **TPNTZ**

\*Advanced Photofunctional Materials Laboratory, Department of Chemistry, Shiv Nadar Institution of Eminence, Delhi NCR, NH-91, Tehsil Dadri, Gautam Buddha Nagar, Greater Noida 201314, Uttar Pradesh, India. Email: debdas.ray@snu.edu.in

†Electronic supplementary information (ESI) available: Synthesis, Characterization, SCXRD, Computational analysis and PL studies provided. CCDC 2441493. See DOI: 10.1039/x0xx00000x



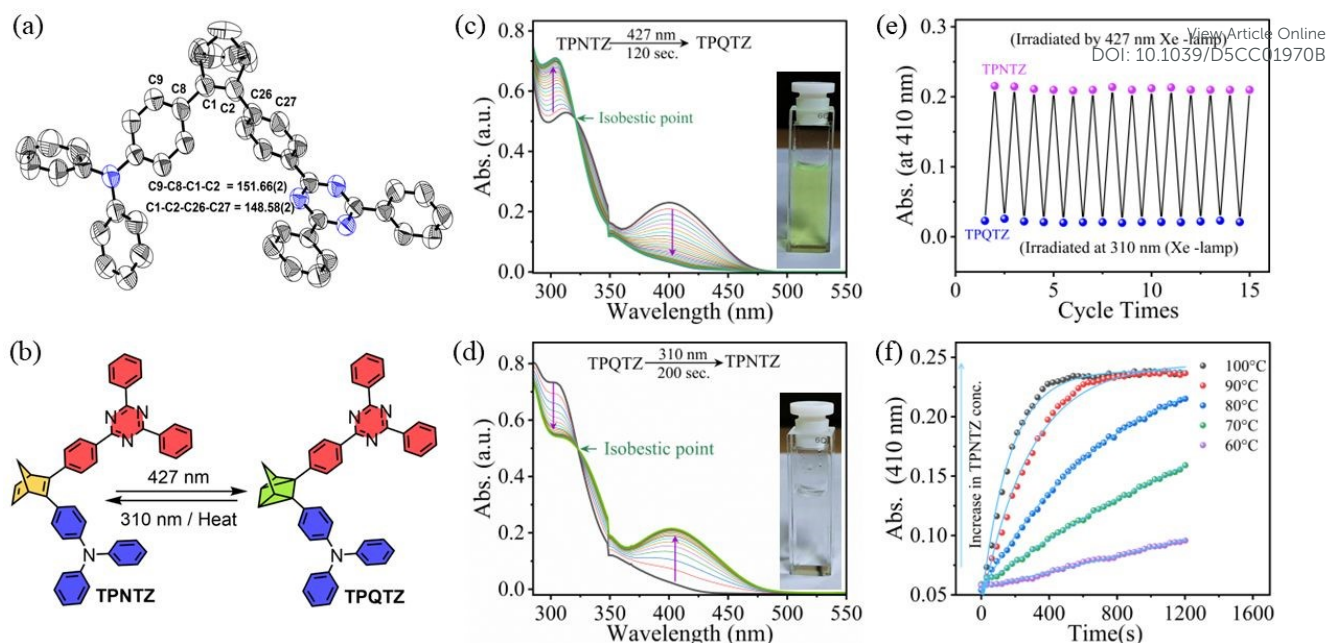


**Fig. 1** (a) Oak Ridge thermal ellipsoid plots (50% probability ellipsoids) showing torsion angles. (b) Two-way photoswitching scheme of **TPNTZ**  $\rightleftharpoons$  **TPQZT**. Absorption spectra in toluene showing photoisomerization of (c) **TPNTZ**  $\rightarrow$  **TPQZT** and (d) **TPQZT**  $\rightarrow$  **TPNTZ**. (e) Reversible switching in toluene under 427/310 nm light. (f) Kinetics plot of the thermal back-conversion from **TPQZT**  $\rightarrow$  **TPNTZ** in toluene at variable temperatures, monitored by the change in absorbance at 410 nm over time.

out of plane, with torsion angles of  $-151.66^\circ$  and  $-148.58^\circ$ , when viewed along the C9–N8–C1–C2 and C1–N2–C26–C27 atoms, respectively (Fig. 1a, Fig. S3a, Table S1, ESI<sup>†</sup>). The donor and acceptor twisted slightly, forming an  $-18.64^\circ$  angle. Adjacent phenyl rings created a  $63.65^\circ$  inter-plane angle (Fig. S3b, ESI<sup>†</sup>). As anticipated, the TNZ core stayed planar ( $0.127 \text{ \AA}$  deviation) and comparable to earlier reported crystals with similar molecular cores.<sup>24</sup> This planar conformation facilitates the formation of linear stacking of TNZ where  $\pi \cdots \pi$  interactions ( $3.635 \text{ \AA}$ ) occur between neighbouring triazine rings and adjacent phenyl rings (Fig. S3c, ESI<sup>†</sup>). Furthermore, as expected, all three phenyl groups of TPA unit are angularly oriented to each other due to the free  $sp^3$ -hybridized nitrogen centre.

We studied the photochromic reaction of **TPNTZ**, tracking its conversion to the metastable **TPQZT** form (Fig. 1b). Absorption measurement of **TPNTZ** in toluene revealed two distinct bands: one at  $315 \text{ nm}$  ( $\epsilon = 5.2 \times 10^4 \text{ M}^{-1}\text{cm}^{-1}$ ) and another at  $410 \text{ nm}$  ( $\epsilon = 2.3 \times 10^4 \text{ M}^{-1}\text{cm}^{-1}$ ) (Fig. 1c). The higher-energy band resulted from a  $\pi\text{-}\pi^*$  transition, while the lower-energy band reflected TBCT. When exposed to  $427 \text{ nm}$  blue light, the  $360\text{--}500 \text{ nm}$  absorbance gradually decreased and stabilized at  $410 \text{ nm}$  ( $\epsilon = 2.5 \times 10^3 \text{ M}^{-1}\text{cm}^{-1}$ ). Simultaneously, an increase was observed in the higher-energy band ( $\epsilon = 7.2 \times 10^4 \text{ M}^{-1}\text{cm}^{-1}$  at  $310 \text{ nm}$ ), leads a colour change from green to transparent, indicating the gradual transformation of **TPNTZ** to **TPQZT** over time (Fig. 1c). The isobestic point at  $322 \text{ nm}$  indicated a well-defined, clean photoisomerization. Using first-order kinetics, we determined the isomerization rate constant in toluene to be  $4.70 \times 10^{-2} \text{ s}^{-1}$  under a photon flux of  $3.9 \times 10^{-9} \text{ mol s}^{-1}$  (Fig. S4a, ESI<sup>†</sup>). To examine reverse photo-isomerization, we irradiated **TPQZT** in toluene with  $310 \text{ nm}$  UV light at its QC-centric absorption band. As **TPQZT** converted back to **TPNTZ**, the higher-energy band started decreasing with an increase in lower-energy band intensity due to increased conjugation (Fig. 1d). Notably, there

are only a few reports where QC-centric absorption activates back-isomerization.<sup>25</sup> The back photoisomerization rate constant in toluene was measured to be  $2.79 \times 10^{-2} \text{ s}^{-1}$  at photon flux of  $2.78 \times 10^{-9} \text{ mol s}^{-1}$  (Fig. S4b, ESI<sup>†</sup>). We calculated the photoisomerization quantum yields ( $\phi$ ) for both processes in various solvents (Fig. S4 and Table S2, ESI<sup>†</sup>). Notably, in toluene,  $\phi(\text{NBD} \rightarrow \text{QC})$  reached  $0.66$  at  $427 \text{ nm}$ , while  $\phi(\text{QC} \rightarrow \text{NBD})$  was  $0.54$  at  $310 \text{ nm}$ , demonstrating efficient reversible photoisomerization. To assess photostability, we irradiated **TPNTZ** solution ( $10 \text{ }\mu\text{M}$ ) with alternating  $427 \text{ nm}$  and  $310 \text{ nm}$  wavelengths for multiple cycles in toluene and MCH; monitoring absorbance at  $410 \text{ nm}$  leads to no significant change in absorbance, confirming high fatigue resistance (Fig. 1e, Fig. S5, ESI<sup>†</sup>). Although this couple shows excellent photo reversibility and high fatigue resistance in dilute solution, it undergoes photodegradation at higher concentrations which is common in NBD- derivatives (Fig. S6, ESI<sup>†</sup>).<sup>11</sup>

Further, we explored charge transfer (CT) characteristics of the **TPNTZ/TPQZT** couple in different solvents. **TPNTZ**'s absorption spectra remained largely unchanged across solvents of different polarities. **TPQZT**, however, showed a redshift in its  $350\text{--}450 \text{ nm}$  low-energy tail and a hyperchromic increase in absorbance as solvent polarity increased. This suggested that stronger dipole stabilization in polar solvents enhanced TSCT from the TPA donor to the TNZ acceptor (Fig. S7, ESI<sup>†</sup>). We analysed the thermal half-life ( $t_{1/2}$ ) of **TPQZT** at RT in toluene by examining its back conversion to **TPNTZ** in toluene at five temperatures (Fig. 1f, Fig. S8, Table S3, ESI<sup>†</sup>).<sup>26</sup> From the Arrhenius plot, we estimated a  $t_{1/2}$  of  $56.5$  hours at  $298 \text{ K}$  with an activation energy of  $93.56 \text{ kJ/mol}$ . The transition state entropy was calculated to be  $41.66 \text{ J K}^{-1} \text{ mol}^{-1}$ , suggesting a moderate energy barrier and a concerted reaction mechanism with a well-ordered transition state. Importantly, the **TPNTZ/TPQZT** switches demonstrated photo-thermal reversible (PTR) switching with outstanding





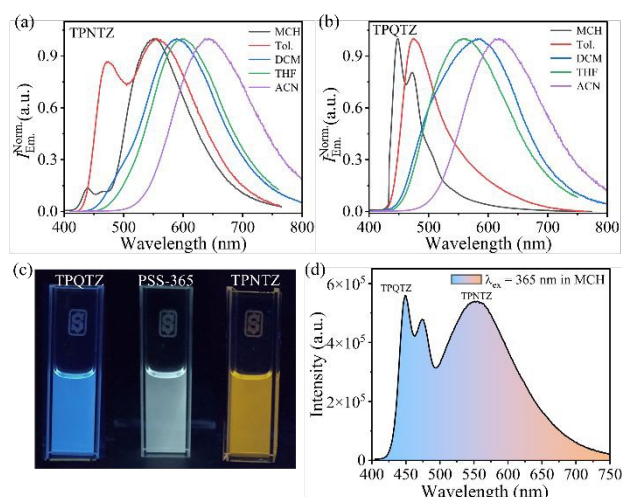


**Fig. 2.** PL spectra of (a) TPNTZ and (b) TPQ TZ with solvents of disparate polarity. (c) Fluorescence photographs of TPQ TZ, PSS-365, and TPNTZ under 365 nm UV-light in MCH. (d) Fluorescence spectra at 365 nm excitation MCH.

fatigue resistance. Even after 20 cycles of irradiation and heating, the material consistently restored its absorbance, highlighting its robustness and thermal stability (Fig. S7c, ESI<sup>†</sup>). Interestingly, as solvent polarity increases, the  $t_{1/2}$  of the TPQ TZ  $\rightarrow$  TPNTZ thermal-back isomerization significantly decreases, suggesting that polar solvents assist CT from donor to acceptor, facilitating the reverse isomerization (Fig. S9, ESI<sup>†</sup>). We studied the emission of TPNTZ and TPQ TZ in solvents with varying polarity. When excited at 410 nm, TPNTZ showed bright yellow-orange emission in MCH with an approximate photoluminescence quantum yield ( $\phi_{\text{PL}}$ ) of 83.4  $\pm$  2%. As polarity increased, emission shifted red and  $\phi_{\text{PL}}$  dropped, confirming CT excited state stabilization (Fig. 2a, Table S3, ESI<sup>†</sup>). TPQ TZ, excited at 310 nm, displayed a blue-shifted emission compared to TPNTZ (Fig. 2b). Importantly, in MCH, TPQ TZ emitted a structured blue emission ( $\phi_{\text{PL}}$  = 24.0  $\pm$  3%), which became broad (red shifted) in polar solvents (Fig. 2b). This suggests that solvent polarity has a stronger effect on TPQ TZ's CT state than on TPNTZ. The measured  $\phi_{\text{PL}}$  reflects both emissions, with each derivative dominating at different excitation wavelengths—410 nm and 310 nm. Earlier studies found that TSCT interactions respond more to solvent polarity than TBCT interactions.<sup>27</sup> TPQ TZ facilitates TSCT because its TPA and TNZ units lack a direct conjugated bond. In contrast, TPNTZ's TPA and TNZ units are covalently linked via an NBD bridge, promoting TBCT. This structural difference makes TPQ TZ more sensitive to solvent polarity. TPQ TZ shows higher  $\phi_{\text{PL}}$  in polar solvents, suggesting solvent-driven CT from TPA to TNZ (Table S3, ESI<sup>†</sup>). Fluorescence decay studies revealed that both isomers had nanosecond decay times in aerated conditions, which increased with solvent polarity, indicating stabilization of the excited state. (Fig. S10, Table S4, ESI<sup>†</sup>). In MCH, TPNTZ emitted orange light at 565 nm, while TPQ TZ emitted blue light at 445 nm (Fig. 2c). We aimed to produce white-light emission by balancing their concentrations. Absorption studies revealed that both TPNTZ and TPQ TZ absorb weakly at 365 nm. Upon irradiation at this wavelength, photoisomerization of TPNTZ was initiated; however, a complete conversion to TPQ TZ did not occur, leading to a photo-stationary state (PSS-365), with TPNTZ

fraction of 0.216, with TPQ TZ/TPNTZ ratio of 3.6:1 (Fig. S11, ESI<sup>†</sup>). Exciting this at 365 nm resulted in white-light emission ( $\phi_{\text{PL}}$  = 44.5  $\pm$  2%), with Commission Internationale de l'Éclairage (CIE 1931) coordinates 0.335, 0.391 (Fig. 2c, d, Fig. S12, ESI<sup>†</sup>). Note that the total quantum yield (fluorescence and photoisomerization) exceeds 100% in MCH and toluene due to combined emission from the TPNTZ/TPQ TZ isomeric pair.<sup>12c,25</sup> Moreover, photoswitching in the 5 wt% TPNTZ-polystyrene blend produced solution-like absorption changes and a visible, reversible color change (Fig. S13, ESI<sup>†</sup>). Irradiation at 410 nm gradually reduced emission at 530 nm, suggesting decreased TBCT during isomerization to TPQ TZ. Switching to 310 nm light restored the emission, confirming fully reversible photoswitching (Fig. S14, ESI<sup>†</sup>).

We analyzed electronic properties of TPNTZ and TPQ TZ using density functional theory (DFT) and time-dependent DFT (TD-DFT) (ESI<sup>†</sup>).<sup>28</sup> In both isomers, FMOs were spatially separated with distinct localization patterns. In TPNTZ, the HOMO is largely localized on the TPA and double bond of NBD and extends somewhat over the first phenyl ring of the TNZ. The LUMO is mainly localized on the TNZ core, with minor contributions from the phenyl ring of TPA attached to the NBD. This significant HOMO-LUMO overlap results in high oscillator strength ( $f$  = 0.5917) (Fig. S15a, ESI<sup>†</sup>). However, in TPQ TZ, the HOMO is predominantly localized to TPA and LUMO on the TNZ unit resulting in a comparatively low oscillator strength ( $f$  = Hole/electron analysis further revealed a contrasting result with TPQ TZ showing a dominant CT character compared to its lower 0.0064) (Fig. S15b, ESI<sup>†</sup>). This distinct separation weakens

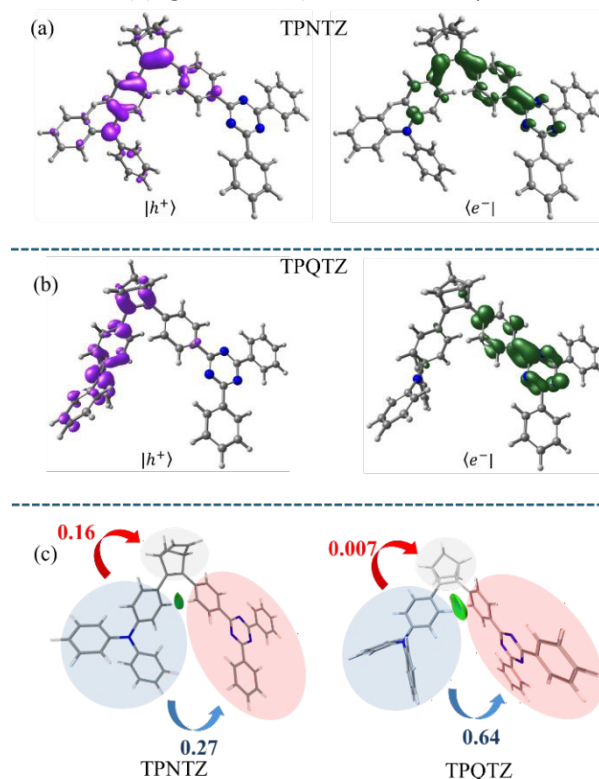


**Fig. 3.** (a) Hole–electron analysis (NTOs: |h<sup>+</sup>⟩, violet; |e<sup>-</sup>⟩, green) for transition corresponding to the S1 and T1 excited states of (a) TPNTZ and (b) TPQ TZ at isosurface values of  $\pm 0.002$  au [M06-2X/6-31g(d,p)]. (c) 3D Visualization of non-covalent interaction and charge transfer amount in TPNTZ and TPQ TZ (left to right); green isosurface refers to interactions.



direct through bond interactions and enhances the possibility of TSCT. energy isomer owing to the well-separated hole and electron densities on the TPA and TNZ, respectively (Fig. 3a, b). Further independent gradient model based on Hirshfield partition of molecular density and inter-fragment charge transfer analyses at optimized S1 geometry confirmed the dominant TSCT (TPA→TNZ) character of the **TPQTZ** (Fig. 3c).<sup>29</sup> In summary, this study explored how structural changes in a photochromic donor-acceptor system control charge transfer. The system switches between through-bond and through-space charge transfer by breaking and reforming a C=C double bond. Photophysical analysis showed controlled isomerization produces white-light emission, revealing new possibilities for optoelectronics.

D.R. acknowledges research funding from the Anusandhan National Research Foundation (ANRF), Department of Science and Technology, India (CRG/2022/000128 and IRG/2024/000038/CS), and Shiv Nadar Institution of Eminence (SNIOE). M.U. and R.D. thank SNIOE for their fellowships. The authors acknowledge the high-performance computing cluster 'MAGUS' at SNIOE for providing computational resources.

## Data availability statements

The data supporting this article have been included as part of the Supplementary Information.

## Conflicts of interest

There are no conflicts to declare.

## Notes and references

- (a) S. Kawata and Y. Kawata, *Chem. Rev.*, 2000, **100**, 1777-1788; (b) V. Adam, H. Mizuno, A. Grichine, J.-i. Hotta, Y. Yamagata, B. Moeyaert, G. U. Nienhaus, A. Miyawaki, D. Bourgeois and J. Hofkens, *J. Biotechnol.*, 2010, **149**, 289-298.
- (a) W. Si, J. Li, G. Li, C. Jia and X. Guo, *J. Mater. Chem. C* 2024, **12**, 751-764.
- F. Höglspurger, B. E. Vos, A. D. Hofemeier, M. D. Seyfried, B. Stövesand, A. Alavizargar, L. Topp, A. Heuer, T. Betz and B. J. Ravoo, *Nat. Commun.*, 2023, **14**, 3760.
- (a) A. Dreos, Z. Wang, J. Udmark, A. Ström, P. Erhart, K. Börjesson, M. B. Nielsen and K. Moth-Poulsen, *Adv. Energy Mater.*, 2018, **8**, 1703401; (b) R. R. Weber, C. N. Stindt, A. M. J. Harten, B. L. Feringa, *Chem. Eur. J.* 2024, **30**, e202400482.
- (a) Z. Yang, P.-A. Cazade, J.-L. Lin, Z. Cao, N. Chen, D. Zhang, L. Duan, C. A. Nijhuis, D. Thompson and Y. Li, *Nat. Commun.*, 2023, **14**, 5639; (b) J. M. Mativetsky, G. Pace, M. Elbing, M. A. Rampi, M. Mayor and P. Samori, *J. Am. Chem. Soc.*, 2008, **130**, 9192-9193.
- (a) B. Shao, N. Stankewitz, J. A. Morris, M. D. Liptak and I. Aprahamian, *Chem. Commun.*, 2019, **55**, 9551-9554; (b) M. D. Johnstone, C.-W. Hsu, N. Hochbaum, J. Andreasson and H. Sunden, *Chem. Commun.*, 2020, **56**, 988-991.
- (a) T. Fukaminato, T. Hirose, T. Doi, M. Hazama, K. Matsuda and M. Irie, *J. Am. Chem. Soc.*, 2014, **136**, 17145-17154; (b) J. Zhang and H. Tian, *Adv. Opt. Mater.*, 2018, **6**, 1701278.
- B. Seefeldt, R. Kasper, M. Beining, J. Mattay, J. Arden-jacob, N. Kemnitzer, K. H. Drexhage, M. Heilemann and M. Sauer, *Photochem. Photobiol. Sci.*, 2010, **9**, 213-220.
- Y. Yokoyama, *Chem. Rev.*, 2000, **100**, 1717-1740.
- (a) H. D. Bandara and S. C. Burdette, *Chem. Soc. Rev.*, 2012, **41**, 1809-1825; (b) F. A. Jerca, V. V. Jerca and R. Hoogenboom, *Nat. Rev. Chem.*, 2022, **6**, 51-69.
- E. E. Bonfantini and D. L. Officer, *Chem. Commun.*, 1994, 1445-1446.
- (a) J. Ko, Y. Yoo, Y. Lee, H. Jeong and Y. Song, *iScience*, 2022, **25**, 104727; (b) M. Upadhyay, R. Deka and D. Ray, *J. Phys. Chem. Lett.*, 2024, **15**, 3191-3196. (c) B. E. Tebikachew, F. Edhborg, N. Kann, B. Albinsson, K. Moth-Poulsen, *Phys. Chem. Chem. Phys.*, 2018, **20**, 23195-23201. (d) S. Ghasemi, et al., *Chem. Eur. J.* 2024, **30**, e202400322.
- J. Orrego-Hernández, A. Dreos and K. Moth-Poulsen, *Acc. Chem. Res.*, 2020, **53**, 1478-1487.
- (a) D. Zhang and M. Heeney, *Asian J. Org. Chem.*, 2020, **9**, 1251-1251; (b) X. Wan, C. Li, M. Zhang and Y. Chen, *Chem. Soc. Rev.*, 2020, **49**, 2828-2842.
- (a) S. Dey, M. Hasan, A. Shukla, N. Acharya, M. Upadhyay, S.-C. Lo, E. B. Namdas and D. Ray, *J. Phys. Chem. C*, 2022, **126**, 5649-5657; (b) H. Noda, X.-K. Chen, H. Nakanotani, T. Hosokai, M. Miyajima, N. Notsuka, Y. Kashima, J.-L. Brédas and C. Adachi, *Nat. Mater.*, 2019, **18**, 1084-1090.
- (a) Z. Zhao, R. Du, X. Feng, Z. Wang, T. Wang, Z. Xie, H. Yuan, Y. Tan and H. Ou, *Curr. Med. Chem.*, 2025, **32**, 322-342; (b) S. Datta and J. Xu, *ACS Appl. Bio Mater.*, 2023, **6**, 4572-4585.
- M. U. Khan, A. Fatima, S. Nadeem, F. Abbas and T. Ahamad, *Polycycl. Aromat. Compd.*, 2024, **44**, 5553-5583.
- B. E. Tebikachew, H. B. Li, A. Pirrotta, K. Börjesson, G. C. Solomon, J. Hihath and K. Moth-Poulsen, *J. Phys. Chem. C*, 2017, **121**, 7094-7100.
- S. Giannini and J. Blumberger, *Acc. Chem. Res.*, 2022, **55**, 819-830.
- J.-T. Ye and Y.-Q. Qiu, *Phys. Chem. Chem. Phys.*, 2021, **23**, 15881-15898.
- (a) S. Kumar, L. G. Franca, K. Stavrou, E. Crovini, D. B. Cordes, A. M. Slawin, A. P. Monkman and E. Zysman-Colman, *J. Phys. Chem. Lett.*, 2021, **12**, 2820-2830; (b) Y. Long, K. Chen, C. Li, W. Wang, J. Bian, Y. Li, S. Liu, Z. Chi, J. Xu and Y. Zhang, *J. Chem. Eng.*, 2023, **471**, 144759.
- (a) S. Dey, R. Deka, M. Upadhyay, S. Peethambaran and D. Ray, *J. Phys. Chem. Lett.*, 2024, **15**, 3135-3141; (b) N. Acharya, M. Upadhyay, S. Dey and D. Ray, *J. Phys. Chem. C*, 2023, **127**, 7536-7545.
- W. J. Yoo, G. C. Tsui and W. Tam, *Eur. J. Org. Chem.*, 2005, 1044-1051.
- (a) S. Kumar, P. Rajamalli, D. B. Cordes, A. M. Slawin and E. Zysman-Colman, *Asian J. Org. Chem.*, 2020, **9**, 1277-1285; (b) H. Tanaka, K. Shizu, H. Nakanotani and C. Adachi, *Chem. Mater.*, 2013, **25**, 3766-3771;
- L. Fei, H. Hölzel, Z. Wang, A. E. Hillers-Bendtsen, A. S. Aslam, M. Shamsabadi, J. Tan, K. V. Mikkelsen, C. Wang and K. Moth-Poulsen, *Chem. Sci.*, 2024, **15**, 18179-18186.
- K. J. Laidler, *J. Chem. Edu.*, 1984, **61**, 494.
- H. Tsujimoto, D.-G. Ha, G. Markopoulos, H. S. Chae, M. A. Baldo and T. M. Swager, *J. Am. Chem. Soc.*, 2017, **139**, 4894-4900.
- M. J. Frisch, et al., Gaussian 16, Revision C.01. 2016, Gaussian Inc., Wallingford, CT, 2016.
- T. Lu and F. Chen, *J. Comput. Chem.*, 2012, **33**, 580-592.



**Data availability statements**

1. The data supporting this article have been included as part of the Supplementary Information.

